ELSEVIER

Biophysical Chemistry 104 (2003) 523–533

Biophysical Chemistry

www.elsevier.com/locate/bpc

Salting-out in the aqueous single-protein solution: the effect of shape factor

Bong Ho Chang, Young Chan Bae*

Division of Chemical Engineering and Molecular Thermodynamics Lab., Hanyang University, Seoul 133-791, South Korea

Received 9 December 2002; received in revised form 10 February 2003; accepted 10 February 2003

Abstract

A molecular–thermodynamic model is developed to describe salt-induced protein precipitation. The protein–protein interaction goes through the potential of mean force. An equation of state is derived based on the generalized van der Waals partition function. The attractive term including the potential of mean force is perturbed by the statistical mechanical perturbation theory. The precipitation behaviors are studied by calculating the partition coefficient with various conditions such as the ionic strength and the shape of protein. Our results show that the protein shape plays a significant role in the protein precipitation behavior.

Keywords: Protein precipitation; Equation of state; Potential of mean force; Protein shape

1. Introduction

In the early days of protein chemistry, the only practical way of separating different types of protein was by causing part of a mixture to precipitate through alteration of some property of the solvent. Precipitation is the simplest and the oldest practical way to separate different proteins from a solution mixture. Separation is achieved through the addition of precipitation agents such as inorganic salts, non-ionic polymers, polyelectrolytes and organic solvents [1–4].

Many research groups have studied the protein precipitation behavior with various experimental techniques. These experimental results suggest that the protein salting-out may be considered a liquid–liquid phase separation resulting in a supernatant fluid phase with a dense precipitate fluid phase. For instance, from Shih et al.'s experiment [3], the solid phase has both solid- and fluid-like behavior and definitely has no long-range order characteristic of protein crystals. In fact, it is now accepted that the dense phase is actually a dense fluid phase. Consequently, most theories for phase equilibrium use the same model for the supernatant fluid and the dense precipitate fluid phases. The degree of separation is characterized by the partition coefficient, K_e, which is defined as the ratio of the protein concentration in the dense phase to that in the supernatant phase. Recent theoretical studies [5–12] have been directed at developing more fundamental models that account for the

*Corresponding author. Tel.: +82-2-2290-0529; fax: +82-2-2296-6280; website: http://www.inchem.hanyang.ac.kr/lab/mtl.

E-mail address: ycbae@hanyang.ac.kr (Y.C. Bae).

0301-4622/03/$ - see front matter
doi:10.1016/S0301-4622(03)00041-3

diverse interactions between the constituents in the protein solution on a molecular level. For example, Mahadevan and Hall [5,6] present a model, based on Baker–Henderson perturbation theory, for the protein precipitation by the non-ionic polymer. Vlachy et al. [7] describe a model for a liquid–liquid phase separation for solutions of colloids and globular proteins, based on the random-phase approximation. However, most recent theoretical studies are concerned with aqueous solutions where the electrolyte concentration is less than 0.1 molar. Experimental studies clearly show that the protein precipitation by salts requires an electrolyte concentration in the range 1–10 molar. Most of authors treat the protein molecules as a large spherical form charged poly-ions.

In this study, we present a molecular–thermodynamic framework for the protein precipitation behavior by highly concentrated inorganic salt. Equation of state is the sum of a hard-sphere reference contribution and a perturbation. The reference term is derived based on the Carnahan–Starling expression [13] and the simple van der Waals-type term is used for the perturbation to describe the effect of protein shape, i.e. the degree of deviation from the sphericity. We also discuss the protein–protein effective two-body potentials. These include potentials that are given by the DLVO theory [14] in addition to an osmotic attraction term to account for the excluded volume effect of salt and also a square-well potential that accounts for all extra forces such as hydrogen bonding forces or possible hydrophobic forces.

2. Theoretical consideration

For the single-protein, the equilibrium model treats the aqueous protein solution (protein, ions and water) as a system of proteins in a continuum pseudosolvent (water and ions). In this case, we assume that the protein–protein interaction plays the primary role in affecting phase separation. Therefore, salt–salt and salt–protein interaction are not treated explicitly.

2.1. The potential of mean force

Protein interactions can be described quantitatively by a two-body potential of mean force; three-body and higher interactions become important at protein concentrations higher than those of reported here.

Kuehner et al. [10] proposed a sum of four potentials of mean force to describe to the overall perturbation potential of mean force, $W_{pp}(r)$, between two different protein molecules;

$$W_{pp}(r) = W_{elec}(r) + W_{disp}(r) + W_{osmotic}(r) + W_{specific}(r) \quad (1)$$

where r is the center-to-center separation. $W_{elec}(r)$ is the electric double-layer-repulsion potential, $W_{dis}(r)$ is the dispersion potential, $W_{osmotic}(r)$ is an attractive interaction due to the excluded-volume effect of the salt ions and is essential to describe phase transitions induced by a non-adsorbing polymer [5,6], however, it may also be important at higher concentrations of simple salts [15]. $W_{specific}(r)$ is an attractive potential between proteins included to represent any specific chemical effects such as hydrophobic interactions. Details are shown in Appendix A.

Fig. 1 shows a representative overall protein–protein perturbation potential of mean force. For $I=0.2$ M (Fig. 1a), The Coulombic repulsion shows positive, while that of $I=8.0$ M (Fig. 1b) is near zero. It means that at higher ionic strength, the electric double-layer potential is negligible due to the strong dielectric screening of Coulombic repulsion. The osmotic attraction acts as a short-range attraction, which is approximated by a solvent diameter. The total potential of $I=8.0$ M is more attractive than that of $I=0.2$ M. This explains that higher ionic strength produces attraction strong enough to yield higher partition coefficients.

2.2. Equation of state

For an aqueous protein solution, we employ a statistical thermodynamic model based on the same fundamental ideas that is the generalized van der Waals partition function. The partition function Q depends on temperature T, system volume V and number of protein molecules N. The generalized van der Waals partition function [16] for a hard sphere fluid is given:

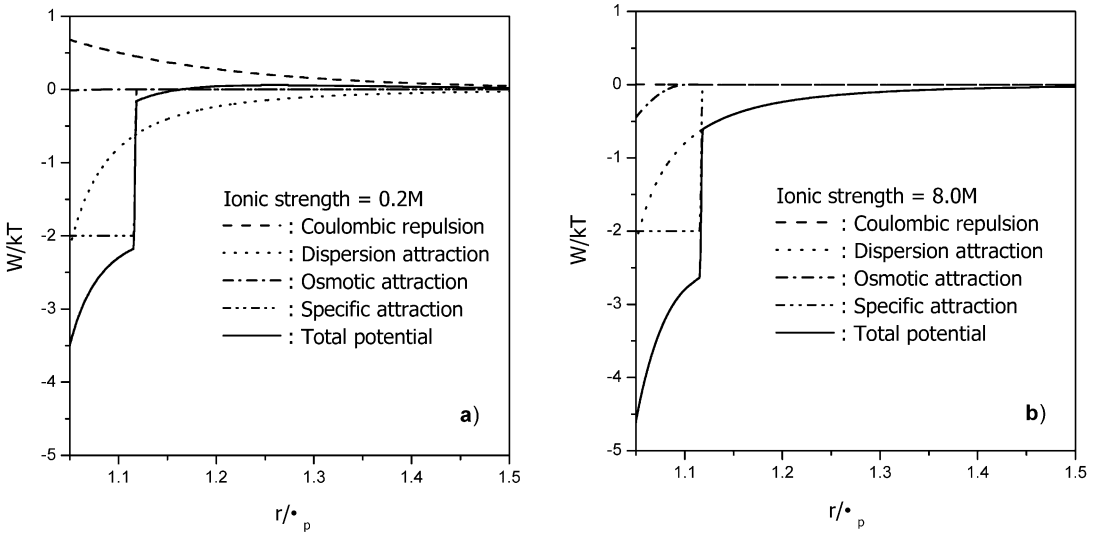

Fig. 1. The contributions to the total potential of mean force as a function of r/σ_p for $I=0.2$ M (a) and $I=8$ M (b).

$$Q(T,V,N)=\frac{1}{N!}\left(\frac{V}{\Lambda^3}\right)^N\left(\frac{V_f}{V}\right)^N\left[\exp\left(\frac{-E_0}{2k_BT}\right)\right]^N(q_{r,v})^N \tag{2}$$

where Λ is the de Broglie wavelength and the free volume V_f is the volume available to the center of mass of a molecule. E_0 is the intermolecular potential energy of one molecule due to the attractive forces from all other molecules. The contribution per molecule from rotational and vibrational degree of freedom, $q_{r,v}$, is a unit $(=1)$ for a perfect sphere molecule. For large molecules, $q_{r,v}$ depends significantly on density, when the molecules deviate from the spherical shape. Donohue [17] proposed the expression of $q_{r,v}$.

$$q_{r,v}(V,T)=\left[\frac{V_f}{V}\exp\left(-\frac{E_0}{2k_BT}\right)\right]^{c-1} \tag{3}$$

where $3c$ is the total number of effective external degree of freedom per molecule. It is well known that shapes of most proteins are not perfectly spherical. In this work, we replace c by τ_{ps} to take into account the effect of protein shape in the partition function, Q. It is assumed that τ_{ps} affects to the potential of mean force and $q_{r,v}$, simultaneously. Eq. (2) is replaced by:

$$\begin{aligned}Q(T,V,N)&=\frac{1}{N!}\left(\frac{V}{\Lambda^3}\right)^N\left(\frac{V_f}{V}\right)^N\left[\exp\left(\frac{-\bar{E}_0}{2k_BT}\right)\right]^N\\&\quad\times\left(\frac{V_f}{V}\exp\left(\frac{-\bar{E}_0}{2k_BT}\right)\right)^{N(\tau_{ps}-1)}\\&=\frac{1}{N!}\left(\frac{V}{\Lambda^3}\right)^N\left(\frac{V_f}{V}\exp\left(\frac{-\bar{E}_0}{2k_BT}\right)\right)^{N\tau_{ps}}\end{aligned} \tag{4}$$

where $\bar{E}_0=\tau_{ps}E_0$, which is the intermolecular potential energy of a non-spherical protein due to the attractive forces from all other proteins. Interacting types of protein molecules affect the intermolecular potential energy between non-spherical proteins. The fact is found in literature [18] that the interacting types between non-spherical molecules affect the intermolecular potential energies. The interacting types are depicted in Fig. 2. Therefore, τ_{ps} reflects the rotational and vibrational contributions per a protein molecule that are affected by the presence of non-spherical proteins. In this work, we assume that the difference between E_0 and $\bar{E}_0$ originated from non-sphericality is mainly due to the additional volume of a non-spherical molecule.

$$\upsilon_{non} = \upsilon_{sph} + \delta\upsilon_{add} = \upsilon_{sph}\left(1 + \frac{\delta\upsilon_{add}}{\upsilon_{sph}}\right) = \upsilon_{sph}\tau_{ps} \quad (5)$$

where υ represents the volume of a protein molecule and subscript 'non', 'sph' and 'add' stand for non-spherical, spherical and additional, respectively. τ_{ps} is defined by the geometric mean of the ratio of σ_{pi} to σ_p:

$$\tau_{ps} = \left(1 + \frac{\delta\upsilon_{add}}{\upsilon_{sph}}\right) \approx \left(\prod_{j=1}^{n}\sigma_{pi}/\sigma_p^n\right)^{\frac{1}{n}} \approx \left(\frac{\sigma_{px}\sigma_{py}\sigma_{pz}}{\sigma_p^3}\right)^{\frac{1}{3}} \quad (6)$$

where $n=3$ due to the experimental accessibility [19,20] and simplicity. x, y and z are three-directional axes, which are shown in Fig. 3 and σ_{pi} is i-directional crytstallographic unhydrated diameter. The larger value of τ_{ps} means that the each directional protein diameter deviates more from the unhydrated hard sphere diameter. When $\tau_{ps}=1$, i.e. a perfect hard sphere, Q reduces to the

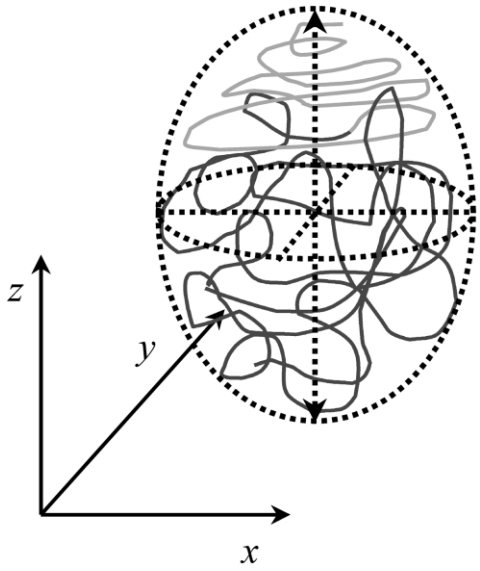

Fig. 3. The three-directional axes for the shape factor of a protein molecule.

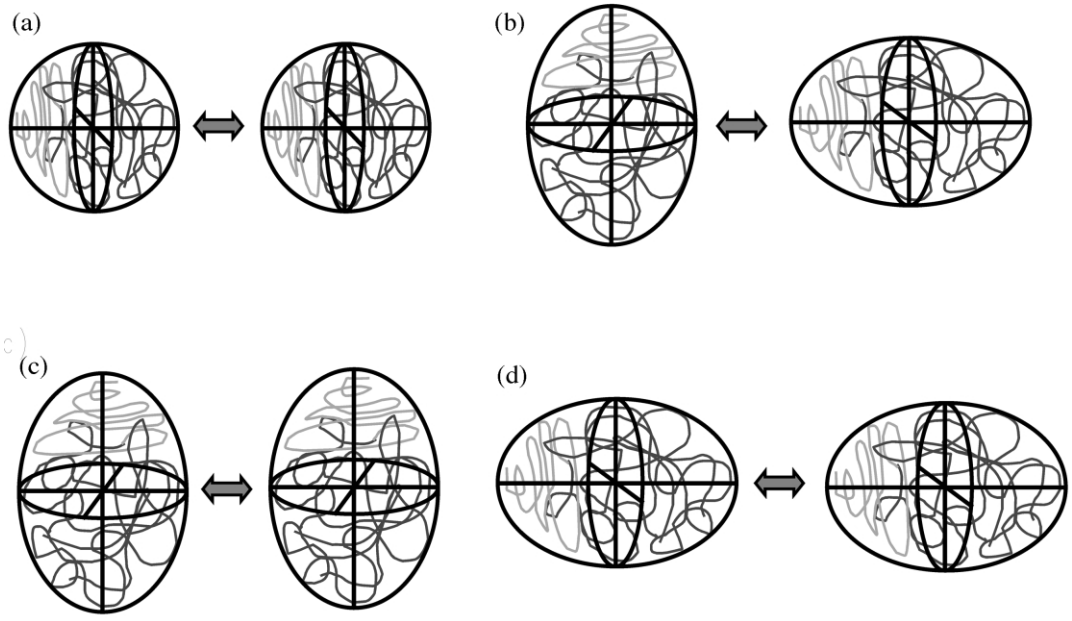

Fig. 2. The interacting types: (a) spherical molecules; (b–d) non-spherical molecules.

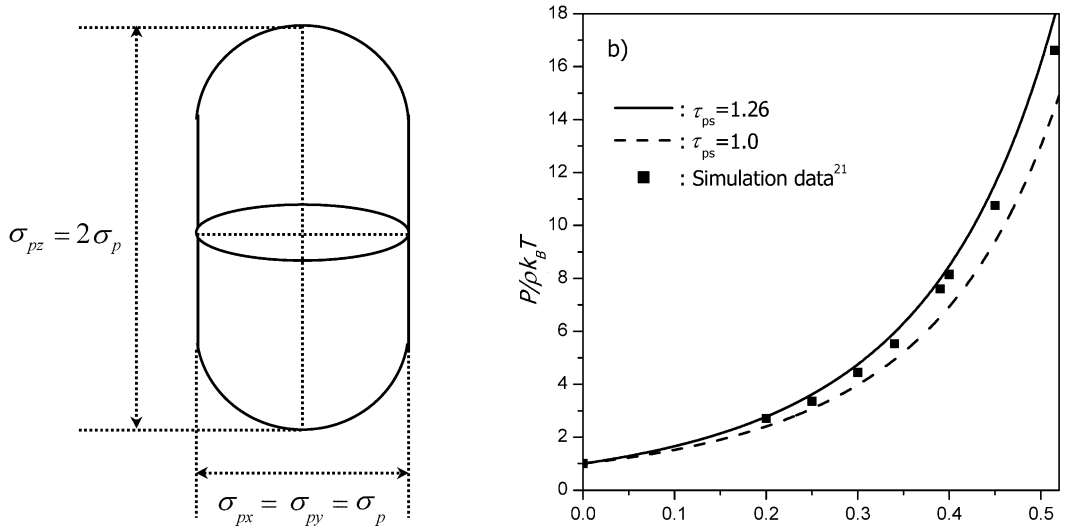

Fig. 4. (a) The three-dimensional shape of the hard prolate spherocylinders [$\gamma(=\sigma_{pz}/\sigma_{px})=2$]. (b) The simulation data of compressibility factors of hard prolate spherocylinders. The solid line is calculated by the proposed reference term. The dashed line is calculated by the Carnahan-Starling reference term.

classical van der Waals-type perturbed-hard-sphere theory.

The equation of state is related:

$$P = k_B T\left(\frac{\partial \ln Q}{\partial V}\right)_{T,N} \tag{7}$$

Substituting Eq. (4) into Eq. (7) with $V_f = V\exp\left[\frac{\eta(3\eta-4)}{(1-\eta)^2}\right]$, Carnahan–Starling expression [13], yields:

$$\left(\frac{P}{\rho k_B T}\right) = 1 + \frac{\tau_{ps}(4\eta-2\eta^2)}{(1-\eta)^3} + \frac{\tau_{ps}^2 \rho U}{2k_B T} \tag{8}$$

where $\rho=(N/V)$ is the number density of protein molecules, P is the pressure. In Eq. (8), τ_{ps}, which results from the third term in Eq. (4), corrects both the underestimated hard sphere contribution and attractive perturbation. Especially, the packing fraction, η, is defined as follows:

$$\eta = \eta_{sph} + \delta\eta_{add} = \frac{\pi\rho\sigma_p^3}{6} \times\left(1+\frac{\delta\eta_{add}}{\eta_{sph}}\right) = \eta_{sph}\tau_{ps} \tag{9}$$

and U is the perturbation energy per unit density,

$$U = \frac{E_0}{\rho} = 4\pi\int W_{pp}(r) r^2 dr \tag{10}$$

where $W_{pp}(r)$ is the sum of the potentials-of-mean-force. We compare the proposed reference term with simulation data [21] of compressibility factors of hard prolate spherocylinders ($\gamma=2$). As shown in Fig. 4a, $\sigma_{px}=\sigma_{py}=\sigma_p$ and $\sigma_{pz}=2\sigma_p$. In this special case, we obtain $\tau_{ps}=1.26$ from Eq. (6). Fig. 4b shows that the proposed model (solid line) gives the better agreement than that of Carnahan–Starling expression (dashed line).

The general equation for calculating the Helmholtz energy from a pressure-explicit equation of state [9] is:

$$\frac{A}{Nk_B T} = \frac{A^0}{Nk_B T} + \int_0^\rho \left(P/\rho 2k_B T - 1\right)\frac{d\rho}{\rho} = \frac{A^0}{Nk_B T} + \frac{\tau_{ps}(4\eta-3\eta^2)}{(1-\eta)^2} + \frac{\rho\tau_{ps}^2 U}{k_B T} \tag{11}$$

where $A^0(T)$ is the Helmholtz energy at standard state.

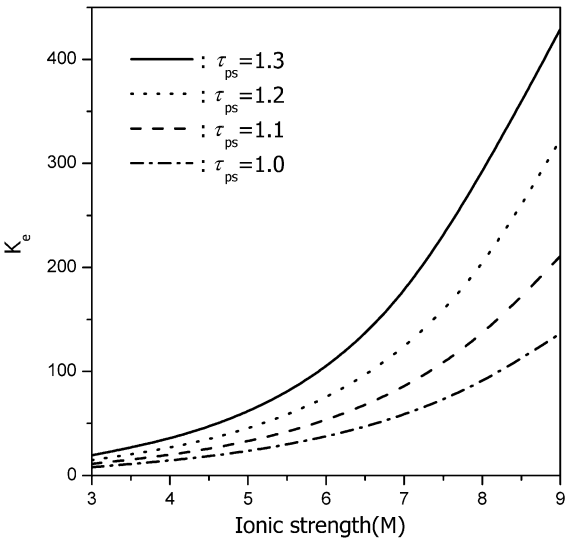

Fig. 5. The effect of ionic strength on partitioning at various τ_{ps} values.

The chemical potential is:

$$\mu = \left(\frac{\partial A}{\partial N}\right)_{T,V} \tag{12}$$

and substituting Eq. (11) into Eq. (12) yields:

$$\frac{\Delta\mu}{k_B T} = \frac{\mu}{k_B T} - \frac{\mu^0}{k_B T} = \frac{\tau_{ps}(8\eta - 9\eta^2 + 3\eta^3)}{(1-\eta)^3} + \ln\rho + \frac{\tau_{ps}^2 \rho U}{k_B T} \tag{13}$$

At equilibrium, protein concentrations in the supernatant and dense-fluid phases are calculated from Eqs. (14) and (15) based on the classical equilibrium conditions:

$$\Delta\mu^s = \Delta\mu^d \tag{14}$$

$$P^s = P^d \tag{15}$$

where superscripts ‘s’ and ‘d’ denote the supernatant and dense phases, respectively.

3. Results and discussion

For the precipitation of a single protein in an aqueous salt solution, we examine the effect of the ionic strength, pH and the protein shape. The partition coefficient, K_e, of the aqueous protein solution can be obtained from the equilibrium conditions and is given by the ratio of the equilibrium number density of protein in the dense phase to that in the supernatant phase [$K = \rho_d/\rho_s = \eta_d/\eta_s$]. For all calculations, the value of z_2(pH) is used from the published experimental data [22,23]. For the hypothetical calculations shown in Figs. 5–8, model parameters are used to correspond to a small globular protein taken to have properties similar to bovine α-chymotrypsin precipitating in ammonium sulfate. Waksman et al. [19] reported that the protein structure change from the supernatant to dense phases is negligible by comparing experimental results of X-ray crystallography and nuclear magnetic resonance (NMR) methods. Therefore, we assume that τ_{ps} of the supernatant phase is the same as that of the dense phase.

Fig. 5 shows the predicted partition coefficient, K_e, plotted as a function of ionic strength for systems with $H/k_BT = 5$, $\varepsilon_{sp}/k_BT = 2$, $\delta = 3$ Å,

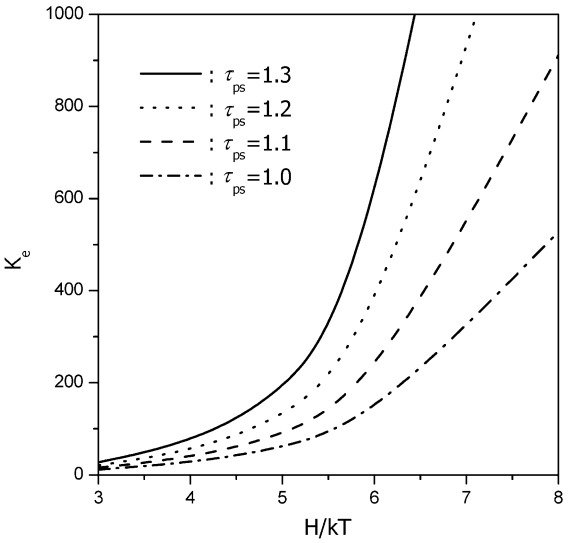

Fig. 6. The effect of the effective Harmaker constant on partitioning at various τ_{ps} values.

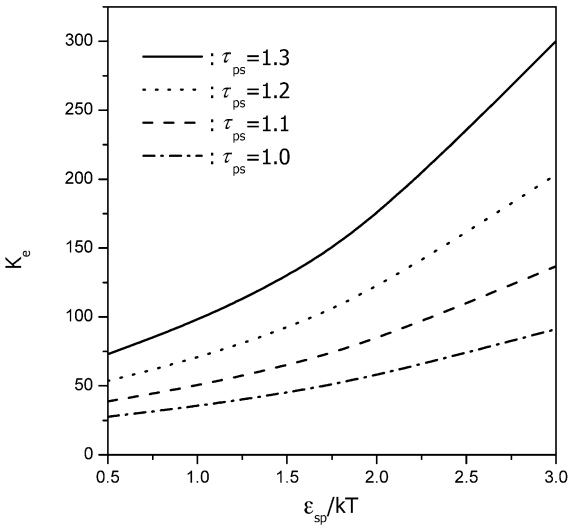

Fig. 7. The effect of ε_{sp}/k_BT on partitioning at various τ_{ps} values.

$\sigma_{ion}=3.5$ Å, pH=8.25, $\sigma_p=34.3$ Å, $\Delta r=0.08$ Å for various values of τ_{ps}. K_e increases exponentially with the ionic strength and is very sensitive to the small change of τ_{ps}. In Fig. 6, K_e is plotted as a function of the effective Hamaker constant at $I=7.0$ for various values of τ_{ps}. The results show that the partition coefficient depends very strongly on the value of H/k_BT. In Figs. 7 and 8, the computed partition coefficient shows relatively weak dependence on ε_{sp}/k_BT and δ. K_e also increases significantly with the small change of τ_{ps}.

Coen et al. [8] have conducted precipitation experiments for two small globular proteins, hen-egg-white lysozyme and bovine α-chymotrypsin, in solutions of ammonium sulfate at various ionic strengths and pH. Figs. 9 and 10 show the two-dimensional structures of bovine α-chymotrypsin and hen-egg-white lysozyme [20], respectively. As shown in these figures, the shapes of two proteins deviate significantly from the spherical type ($\tau_{ps}=1$). Based on the simulated structure, we could calculate τ_{ps} of hen-egg-white lysozyme ($\tau_{ps}=1.62$, Fig. 10) and of bovine α-chymotrypsin ($\tau_{ps}=1.22$, Fig. 9) from Eq. (6). Fig. 11a,b shows experimental and calculated values of K_e as a function of ionic strength for α-chymotrypsin at pH=5.5 and 8.3, respectively. The solid line in Fig. 11a is calculated with $\tau_{ps}=1.22$ that is determined from the simulated structure shown in Fig. 9. From these calculations, τ_{ps} has the larger value at lower pH and higher I. It means that the shape of protein depends strongly on the solvent conditions such as ionic strength, pH, etc. As the ionic strength increases and pH decreases, the salts and acids added in the solution makes the protein molecules more denatured or de-folded. It results in the value of τ_{ps} increases. The model parameters are $H/k_BT=4$, $\varepsilon_{sp}/k_BT=0.5$, $\delta=3$ Å, $\sigma_{ion}=3.5$ Å, $\sigma_p=43.4$ Å and $\Delta r=0.08$ Å, respectively. The small value of H/k_BT is chosen to minimize the effect of H/k_BT on protein precipitation.

Fig. 12 represents the hen-egg-white lysozyme precipitation data in ammonium sulfate solution at pH=4.0 (Fig. 12a) and 8.0 (Fig. 12b) for K_e as a function of ionic strength. Solid line in Fig. 12a represents K_e values at $\tau_{ps}=1.62$ that is calculated from the simulated structure shown in Fig. 10. As shown in these figures, τ_{ps} is the characteristic function of pH and I implicating the nature of each protein molecule. As expected, these calculation results show that the values of τ_{ps} of α-chymotrypsin are smaller than those of hen-egg-white lysozyme. The model parameters are $H/k_BT=4$, $\varepsilon_{sp}/k_BT=1.0$, $\delta=3$ Å, $\sigma_{ion}=3.5$

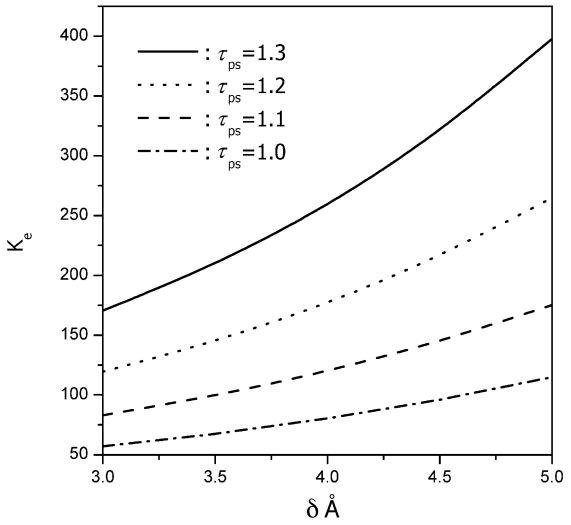

Fig. 8. The effect of δ on partitioning at various τ_{ps} values.

Fig. 9. The two-directional structures of an α-chymotrypsin molecule. The circle is not exact size but a conceptual one. $\sigma_p = 43.4$ is suggested by Kuehner et al. [12].

Å, $\sigma_p = 34.3$ Å and $\Delta r = 0.08$ Å, respectively. Larger ε_{sp}/k_BT value than that of α-chymotrypsin is used as suggested by Kuehner et al. [10].

In the comparison calculated values with experimental data, K_e could be determined by the other parameters, for instance, H/k_BT, ε_{sp}/k_BT and δ.

Fig. 10. The two-directional structures of a hen-egg-white lysozyme molecule. The circle is not exact size but a conceptual one. $\sigma_p = 34.3$ is suggested by Coen et al. [9].

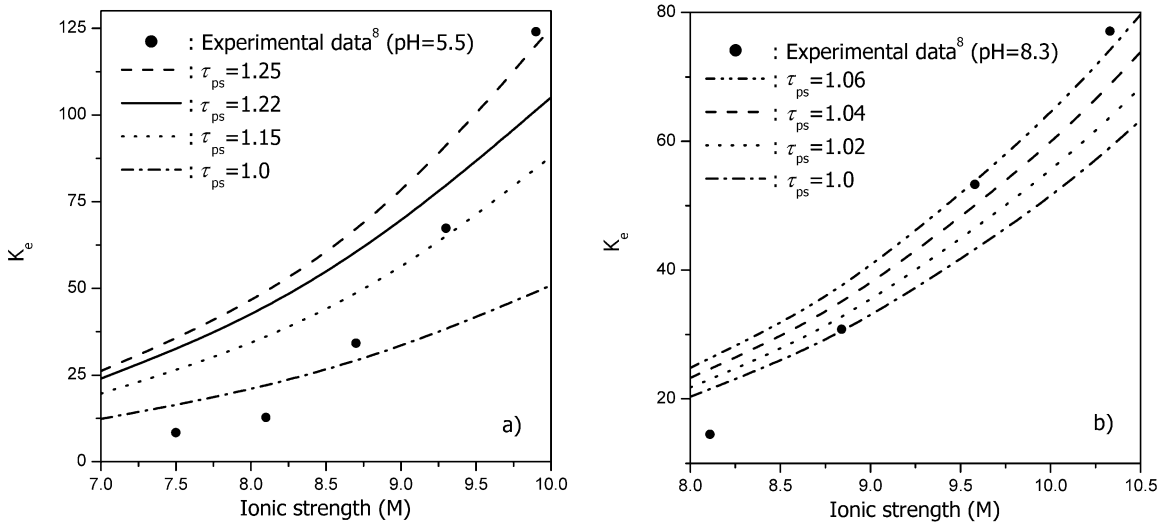

Fig. 11. The partition coefficient, K_e of α-chymotrypsin in ammonium sulfate solution at pH=5.5 (a) and pH=8.3 (b). The dark circles are experimental data and the lines are calculations.

However, it is well known that H/k_BT does not depend on pH and I. It depends on the composition and density of the protein and the chemical nature of the solute [18]. Therefore, most proteins have the similar values of H/k_BT [11,18,24]; nevertheless, many researchers reported the different values of H/k_BT for proteins. It is because, in their calculations, the excluded-volume contribution is underestimated due to assuming that a protein molecule is a perfectly equivalent sphere [22]. In our case, we use the same value of $H/k_BT(=4)$ for α-chymotrypsin and hen-egg-white lysozyme.

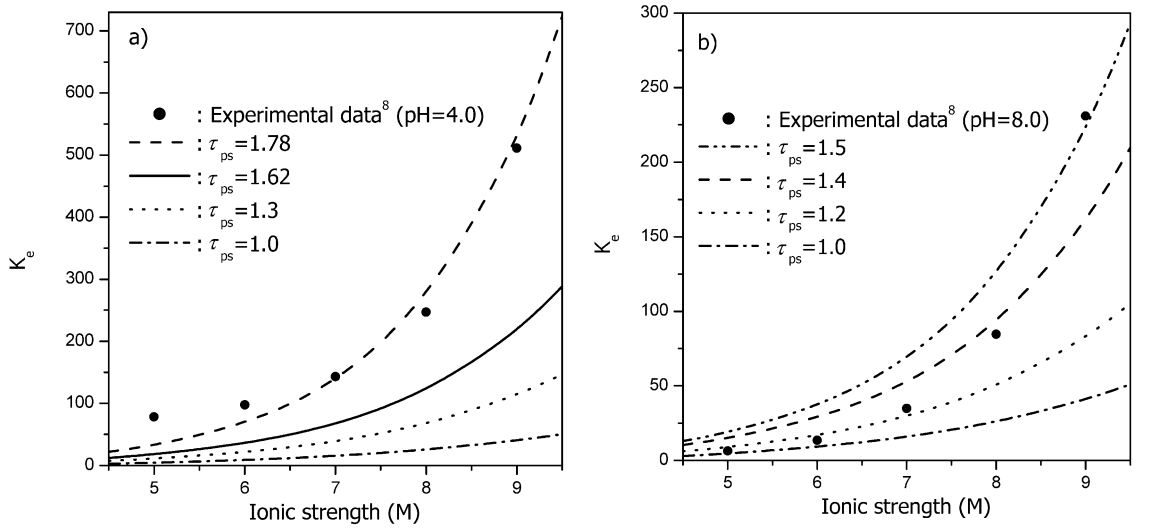

Fig. 12. The partition coefficient, K_e of hen-egg-white lysozyme in ammonium sulfate solution at pH=4.0 (a) and pH=8.0 (b). The dark circles are experimental data and the lines are calculations.

It is reasonable because the underestimated excluded volume contribution is corrected by introducing the protein shape factor, τ_{ps}. In addition, the dependence of ε_{sp}/k_BT and δ on K_e is not more significant than that of τ_{ps} as shown in Figs. 7 and 8. Consequently, τ_{ps} plays as a significant factor in the protein precipitation process.

4. Conclusion

We proposed an approximate equation-of-state model for the salt-induced protein precipitation with the reference term derived from the Carnahan–Starling expression and the perturbation term based on effective potentials of mean force. Especially, the effect of protein shape, τ_{ps}, deviated from sphericity is seriously considered. Calculation results show that at the lower pH and higher I, the structure of protein deviates more from the sphericity so that it gives the higher probability of protein denature or de-folding. The partition coefficient, K_e, increases significantly with the small change of τ_{ps}.

Acknowledgments

The authors are grateful to Prof. J.M. Prausnitz for the discussion on the subject.

Appendix A: The overall potentials

$$W_{elec}(r)=\frac{(z_2e)^2\exp[-\kappa(r-\sigma_p)]}{4\pi\varepsilon_0\varepsilon_r r(1+\kappa\sigma_p/2)^2}$$

for $r > (\sigma_p+2\Delta r)$ (A1)

$$\kappa^2=(2e^2N_aI)/(k_BT\varepsilon_0\varepsilon) \quad \text{(A2)}$$

$$I=(z_{an}^2c_{an}+z_{cat}^2c_{cat})/2 \quad \text{(A3)}$$

$$W_{disp}(r)=-\frac{H}{12}\left[\frac{\sigma_p^2}{r^2}+\frac{\sigma_p^2}{r^2-\sigma_p^2}+2\ln\left(1-\frac{\sigma_p^2}{r^2}\right)\right]$$

for $r>\sigma_p+2\Delta r$ (A4)

$$W_{osmotic}(r)=-\frac{4}{3}\pi\sigma_{ps}^3(\rho_sk_BT)\left[1-\frac{3r}{4\sigma_{ps}}+\frac{r^3}{16\sigma_{ps}^3}\right]$$

for $\sigma_{ps} < r < 2\sigma_{ps}$

$$W_{osmotic}(r)=0 \quad \text{for} \quad r>2\sigma_{ps} \quad \text{(A5)}$$

$$\sigma_{ps}=(\sigma_p+\sigma_{ion})/2 \quad \text{(A6)}$$

$$\sigma_{ion}=(z_{an}\sigma_{cat}+z_{cat}\sigma_{an})/(z_{cat}+z_{an}) \quad \text{(A7)}$$

$$W_{specific}(r)=-\varepsilon_{sp} \quad \text{for} \quad \sigma_p<r<(\sigma_p+\delta)$$

$$W_{specific}(r)=0 \quad for \quad r>(\sigma_p+\delta) \quad \text{(A8)}$$

r	the center to center separation
z_2	the valence of the protein
e	the unit of electron charge
$4\pi\varepsilon_0$	the dielectric permittivity of free space
σ_p	the unhydrated hard-sphere diameter
ε_r	the relative dielectric permittivity of water
Δr	the effective-sphere hydration/stern layer
κ	the inverse of the Debye length
N_a	Avogadro's number
I	the ionic strength of the salt
z_{an}, z_{cat}	the anion and cation valences
c_{an}, c_{cat}	the ionic molar concentrations
H	the effective Hamaker constant for the protein-protein interaction
ρ_s	the total ionic number density
ε_{sp}, δ	model parameters

References

[1] P.R. Foster, P. Dunhill, M.D. Lilly, The precipitation of enzymes from cell extractions of Saccharomyces cerevisiae by polyethylene-glycol, Biochem. Biophys. Acta 317 (1975) 505–516.
[2] R.N. Haire, W.A. Tisel, J.C. White, A. Rosenberg, On the precipitation of proteins by polymers: the hemoglobulin-polyethylene, Biopolymers 23 (1984) 2761–2779.
[3] Y.C. Shih, H.W. Blanch, J.M. Prausnitz, Some characteristics of protein precipitation by salts, Biotech. Bioeng. 40 (1992) 1155–1164.
[4] F. Rothstein, in: R.G. Harrion (Ed.), Protein Precipitation Process Engineering, Dekker, New York, 1994.
[5] H. Mahadevan, C.K. Hall, Statistical–mechanical model of protein precipitation by nonionic polymer, Am. Inst. Chem. Eng. J. 36 (1990) 1517–1528.
[6] H. Mahadevan, C.K. Hall, Theory of precipitation of protein mixtures by nonionic polymer, Am. Inst. Chem. Eng. J. 38 (1992) 573–591.

[7] V. Valchy, H.W. Blanch, J.M. Prausnitz, Liquid–liquid phase separation in aqueous solutions of globular proteins, Am. Inst. Chem. Eng. J. 39 (1993) 215–223.
[8] C.J. Coen, H.W. Blanch, J.M. Prausnitz, Salting-out of aqueous proteins: phase equilibria and intermolecular potentials, Am. Inst. Chem. Eng. J. 41 (1995) 996–1004.
[9] Y.C. Chiew, D.E. Kuehner, H.W. Blanch, J.M. Prausnitz, Molecular thermodynamics of salt-induced protein precipitation, Am. Inst. Chem. Eng. J. 41 (1995) 2150–2159.
[10] D.E. Kuehner, H.W. Blanch, J.M. Prausnitz, Salt-induced protein precipitation: phase equilibria from an equation of state, Fluid Phase Equlibria 116 (1996) 140–147.
[11] D.E. Kuehner, C. Heyer, C. Rämsch, U.M. Fornefeld, H.W. Blanch, J.M. Prausnitz, Interactions of lysozyme in concentrated electrolyte solutions from dynamic light scattering measurements, Biophys. J. 73 (1997) 3211–3224.
[12] R.A. Curtis, A. Montaser, J.M. Prausnitz, H.W. Blanch, Protein–protein and protein–salt interactions in aqueous protein solutions containing concentrated electrolytes, Biotech. Bioeng. 57 (1998) 11–21.
[13] N.F. Carnahan, K.E. Starling, Equation of state for nonattracting rigid spheres, J. Chem. Phys. 51 (1969) 635–636.
[14] E. Verwey, J. Overbeek, Theory of Stability of Lyophobic Colloids, Elsevier, Amsterdam, 1948.
[15] V. Vlachy, J.M. Prausnitz, Donnan equilibrium: hypernetted-chain study of one-component and multicomponent models for aqueous polyelectrolyte solutions, J. Phys. Chem. 96 (1992) 6465–6469.
[16] P. Vimalchand, D. Donohue, Comparison of equation of state for chain molecules, J. Phys. Chem. 93 (1989) 4355–4360.
[17] M.D. Donohue, J.M. Prausnitz, Perturbed hard chain theory for fluid mixtures: thermodynamic properties for mixtures in natural gas and petroleum technology, Am. Inst. Chem. Eng. J. 24 (1978) 849–860.
[18] J.N. Isrelachvlili, Intermolecular and Surface Forces, Academic Press, London, 1985.
[19] G. Waksman, T.S. Krishna, C.H. Williams, J. Kuriyan, Crystal structure of *Escherichia coli* thioredoxin reductase refined at 2 Å resolution, J. Mol. Biol. 236 (1994) 800–816.
[20] Data Bank in National Center for Biotechnology Information, http://www.ncbi.nlm.nih.gov/.
[21] T. Boublik, in: J.V. Sengers (Ed.), Equation of State for Fluid and Fluid Mixtures, 5, Elsevier, Amsterdam, 2000, p. 155.
[22] Y.U. Moon, R.A. Curtis, C.O. Anderson, H.W. Blanch, J.M. Prausnitz, Protein-protein interactions in aqueous ammonium sulfate solutions: lysozyme and bovine serum albumin (BSA), J. Solution Chem. 29 (2000) 699–717.
[23] C.A. Haynes, K. Tamura, H.R. Kröfer, H.W. Blanch, J.M. Prausnitz, Thermodynamic properties of aqueous α-chymotrypsin solutions from membrane osmometry measurements, J. Phys. Chem. 96 (1992) 905–912.
[24] H.C. Hamaker, The London–van der Waals attraction between spherical particles, Physica IV 10 (1937) 1058–1072.